Chapter 2 – SEDIMENT TRANSPORT MECHANISM

Chapter 2

SEDIMENT TRANSPORT MECHANISM

2.1 Introduction

The stability and transport of sediments is central to the analysis and prediction of environmental quality and impact, habitat stability, public health risks, as well as to marine hazards such as ship grounding, access to ports, seabed scouring, siltation of harbors, infill of reservoirs and artificial lakes and in coastline protection. Such issues are addressed worldwide, and of great commercial, aesthetic, social, and scientific importance owing to the sustainable development and coastal zone management. Sediment transport is the mechanism by which coastal erosion proceeds. By understanding coastal sediment transport, we begin to understand and perhaps more effectively manage this global problem.

The land water interface along the coastline is always in a highly dynamic state and nature works towards maintaining an equilibrium condition. The energy due to tide, waves, wind and currents is constantly working in the coastal zone. It requires enough space to dissipate this energy, which is often provided by the beaches, mudflats, marshes and mangroves. Human use of the coasts also requires space and herein lays the conflict, which results in unsustainable coastal systems. The process induces coastal erosion, sediment transport and accretion. However, the major problem is that energy input varies over time and space. The short-term oscillations due to storms/cyclones or long term trend due to sea-level changes also complicates the issue. Therefore, sediment transport in the coastal zone is physical phenomenon, which is highly unpredictable and is a challenge to coastal scientists. It is very crucial to understand the nearshore physical system, the consequent impact on sediment dynamics, and the coastline's response to it.

2.2. Forces triggering the sediment transport

Water covers 71 percent of the Earth. And thus the water of the oceans absorbs a large part of the sun's radiant energy that is not reflected back into space. This absorbed energy warms the water, which in turn warms the air above the oceans, and forms air currents caused by difference in the air temperature. These air currents blow across the water, returning some energy to the water by generating wind waves. The waves then travel across the oceans until they reach the land where their remaining energy is expended on the shore. The motion of the sea, which contributes, to the beach and nearshore dynamical system includes waves, tides, currents, storms, and tsumani.

The beach and nearshore zone of a coast is the region where the forces of the sea react against the land. The dynamical system within this region is composed primarily of the motion of the sea, which supplies energy to the system, and the shore, which absorbs this energy. Because the shoreline is the intersection of the air, land and water, the physical interactions that occur in this region are unique, very complex and difficult to fully understand. As a consequence, a large part of the understanding of the beach and nearshore dynamics is descriptive in nature.

Five groups of processes are primarily responsible for initiating sediment transportation: changes in water level, tides, waves, currents, stream outflow etc.

2.2.1. Changes in water level

Sea-level changes are long-term fluctuations (hundreds or thousands of years or longer) of water level in a coastal zone. The two reasons for sea-level changes are:

- Tectonic - uplift or sinking of a landmass. The actual amount of water in the ocean does not change, however an uplift or sinking of a portion of coast (or ocean bottom) shifts the shoreline up or down.
- Eustatic - increase or decrease of the amount of water in the ocean. Major reason for such an increase or decrease is glaciations, like the Pleistocene Ice Age.

Sea-level changes create emergence and submergence of coastlines that start erosion, which causes sediment transportation.

2.2.2. Tides

Tides are oscillations of ocean waters due to the gravitational forces exerted by the Moon and the Sun upon the oceans. The rising tide is usually referred to as flood, whereas falling tide is called as ebb tide. Tidal currents are the horizontal water movements corresponding to the rise and fall (flood & ebb) of the tide.

High tides are the highest when the Earth, Moon and Sun are all lined up, about every two weeks. Such tides are known as spring tides. When the Moon is perpendicular to the Earth - Sun line (also about every two weeks), high tides are the lowest, called neap tides.

Tides move enormous amount of water four times a day, yet the topographic effect of tides on the coastal zone is small because of their relatively low speeds. In narrow bays and passages, tides move quickly forming so called tidal currents. Tidal currents are capable of erosion. In well-sheltered Gulfs and estuaries tides lose their speed and deposit the fine material (clay, silt) tidal waters carry. Thus bays slowly turn into mud flats, then to marshes.

The gravitational force of the Moon, and to a lesser extent, the Sun, creates tides. These forces of attraction and the fact that the Sun, Moon and Earth are always in motion relative to each other, cause waters of the ocean basin to be set in motion. These tidal motions of water masses are a form of very long period wave motion resulting in a rise and fall of the water surface at a point. There are normally two tides per day, but some localities have only one per day. Tides constantly change the level at which waves attack the beach.

The tidal currents and surges sometimes play an important role in the nearshore dynamical system. When water in one area becomes higher than in another area, water from the higher elevation flows towards the lower level, creating a current. Significant current generated by tides occurs at inlets of lagoons and bays or at entrances to harbors. Tidal current in these constricted places flow in when the tide is rising (flood tide) and flow out as the tide falls (ebb tide).

2.2.3. Waves

Idealized waves of sinusoidal form have wavelength (length between successive crests), height (vertical difference between trough and crest), steepness (ratio of height to length), amplitude (half the wave height), period (length of time between successive waves passing a fixed point) and frequency (reciprocal of period). Water waves show cyclical variations in water level (displacement), from –a (amplitude) in the trough to +a at the crest. Displacement varies not only in space (one wavelength between successive crests) but also in time (one period) between crests at one location). Steeper waves depart from the simple sinusoidal model, and more closely resemble a trochoidal wave form.

Most sea-surface waves are wind-generated. The stronger is the wind, the larger is the wave, so variable winds produce a range of wave sizes. A constant

wind speed produces a fully developed sea, with waves of $H_{1/3}$ (average height of 33% of the waves) characteristic of that wind.

Waves of different wavelengths become dispersed, because those with greater wavelengths and longer periods travel faster than smaller waves. Wave energy is proportional to the square of the wave height, and travels at the group speed. Wave power is the rate of supply of wave energy, and so it is wave energy multiplied by wave speed, i.e. it is wave energy propogated per second per unit length of wave crest (or wave speed multiplied by wave energy per unit area).

Dissipation of wave energy (attenuation of waves) results from white-capping, friction between water molecules, air resistance, and non-linear wave-wave interaction. Waves in shallow water dissipate energy by frictional interaction with the seabed and by breaking. Waves in shallow water may be refracted. In general, steeper the wave and the shallower the beach, the further offshore dissipation begins.

As waves enter the shallow zone, friction against the sea bottom slows wave propagation, especially closer to the bottom. Waves become higher and steeper, tilt forward and, finally, break in a swash as water runs up the beach slope. Thus the energy of circular oscillation is translated into the energy of forward movement. Such waves are called as waves of translation. Backwash is a reversed flow fed by retreating swash.

In the open sea, waves travel more or less as straight lines. However, when a wave enters shallow water, an irregularity in depth bend the wave front as it is slowed down in shallower areas and continues to travel fast in deeper areas. Bending of a wave due to differential speed of travel is called wave refraction.

Although almost all waves are due to wind, occasionally waves are created by undersea tectonic or volcanic events, like an earthquake or massive lava flows in a mid-oceanic rift zone. Such waves are called seismic sea waves or tsunamis. They are characterized by extremely long wavelength and high waves (up to 30 m) once they get to the coastline. These long-period waves can travel across entire oceans at speed exceeding 800 kilometers per hour. Tsunamis can cause extensive damage at times, but fortunately major tsunamis do not occur frequently.

2.2.4. Currents

The primary driving force behind ocean currents is constant winds (for example, trade winds drive the equatorial current). Wind creates currents as it blows over the water surface, producing a stress on the surface water particles and starting the movement of the water particles in the direction in which the wind is blowing. Thus, a surface current is created. When the surface current reaches a carrier, such as the coast, water tends to pile up against the land.

Of all currents, those that flow near coasts have substantial effect on coastal landforms. The most important type of current in the coastal zone is alongshore current. Longshore current ("along the shore") is a current that flows in shallow water, parallel to the shoreline, generally downwind. Longshore currents transport sediments along coasts, sometimes they are powerful enough to erode sea bottom.

2.2.5. Stream outflow

Streams and rivers are important for two reasons. First, they often build deltas that are coastal landforms. Delta is a depositional landform created at the mouth of a river, where flow velocity suddenly drops and most of the river's

sediment is laid down. Secondly, they supply sediments to coasts. Coastal processes, such as waves, tides and currents, then redistribute these sediments.

2.3 Coastal response to natural forces

The shoreline, the intersection of the land and the sea, is where tides, winds, and waves attack the land; and it is where the land responds to this attack by a variety of “give and take” measures, which effectively dissipate the sea’s energy. The areas, most directly affected by the forces of the sea, are the beaches, the gulfs, and the nearshore zone regions that experience the full impact of the sea’s energy.

There are two general types of dynamic beach response to wave motion: response to normal condition and response to storm condition. Normal conditions prevail most of the time, and the wave energy is easily dissipated by the beach’s natural defense mechanisms. However, when storm conditions generates waves containing increased amounts of energy, the coast must respond with extraordinary measures, such as sacrificing large section of beach and dune. In time, the beach may recover, but often not without a permanent loss. Following the storm there is a return to more normal conditions which are dominated by low, long swells. These waves transport sand from the offshore bar, built during the storm and place the material on the beach. Alternate erosion and accretion may be seasonal on some beaches; the winter storm waves erode the beach, and the summer swell (waves) rebuilds it.

Another nearshore dynamical system is littoral transport that is defined as the movement of sediments in the nearshore zone by waves and currents. Littoral transport is divided into two general classes: transport parallel to the

shore (longshore transport) and transport perpendicular to the shore (onshore-offshore transport). The material that is transported is called littoral drift. Onshore-offshore transport is determined primarily by wave steepness, sediment size and beach slope. In general, steep slope waves move more material offshore, and low waves of long period move material onshore.

Longshore transport results from the stirring up of sediment by the breaking wave and the movement of this sediment by both the components of the wave energy in an along shore direction and the longshore current generated by the approaching waves. The direction of longshore transport is directly related to the direction of wave approach and the angle of the wave (crest) to the shore. Thus, due to variability of the wave approach, longshore transport direction can vary from season to season, day to day or hour to hour.

Because reversal in transport direction occurs, and because different types of waves transport material at different rates, two components of longshore transport rate become important. The first is net rate, the net amount of material passing a particular point in the predominant direction during an average year. The second component is gross rate, the total of all material moving past a given point in a year regardless of direction. Most shores consistently have a net annual longshore transport in one direction. The rate depends on the local shore conditions and shore alignment, as well as the energy and direction of wave approach.

Although a beach may be temporarily eroded by storm waves and later partly or wholly restored by swells, and erosion and accretion patterns may occurs seasonally, the long-range condition of the beach-whether eroding, stable, or accreting- depends on the rates of supply and loss of littoral material. The shore accretes or progrades when the rate of supply exceeds the rate of loss. The shore is considered stable (even though subject to storms and seasonal changes) when the long-term rates of supply and loss are equal. Thus

conservation of sand is an important aspect. If coast is unable to respond sufficiently to the natural forces, then erosion occurs.

2.4 Processes of Sediment Transport

2.4.1 Factors controlling the movement of sediment

The four modes of particle transport in water are sliding, rolling, saltation and suspension. Sliding particles remain in continuous contact with the bed, merely tilting to and fro as they move. Rolling grains also remains in continuous contact with the bed, whereas saltation grains 'jump' along the bed in a series of low trajectories. Sediment particles in these three categories collectively form the bedload. The suspended load consists of particles in suspension, that is, particles that follow long and irregular paths within the water and seldom come in contact with the bed until they are deposited when the flow slackens. Sliding and rolling are prevalent in slower flows, saltation and suspension in faster flows. The region of flow influenced by proximity to the surface is called the boundary layer. A boundary layer develops wherever a fluid moves over a surface, whether it is water over the sea bed, or winds over the sea surface.

The friction between flowing water and the seabed generates a boundary layer in which turbulent flow is dominant, except very close to the bed. Movement of sediment (erosion) occurs when the shear stress generated by the frictional force of water flowing over the sediment overcomes the force of gravity acting on the sediment grains and the friction between the grains and the underlying bed. Shear stress is proportional to the square of the mean current speed (and to the density of the water). Movement of grains of a given size begins when the shear stress at the bed reaches a critical value (critical shear stress).

Cohesive sediments contain a high proportion of fine-grained clay minerals and are more difficult to erode than non-cohesive sediments, which often consist mostly of quartz grains. For cohesive sediments, the smaller the particle size, the greater the current speed required to erode them. Once in suspension, clay particles are transported for long distances by the currents that would be much too weak to erode them.

Shear stress is proportional also to the velocity gradient in the boundary layer and to the viscosity of the water. When current speed is plotted against the height above the sea bed (as the vertical axis) on a log-linear graph, the inverse velocity gradient d log z / du is linear. The slope of the line can be used to calculate the shear velocity, and the intercept of the line with the depth axis gives a measure of the bed roughness length (z_o) which increases as the sediment grain size increases; roughness length will also be greater if there are bed forms such as sand ripples.

Figure 2.1 illustrates the relationship between average particle sizes of sediments and the current speeds above, which they are transported (whether in suspension or in the bed load), and below which sediments are deposited. The broken line, indicates that the transition between these two modes of transport is gradational, on account of inherent variability of natural sediments and real currents.

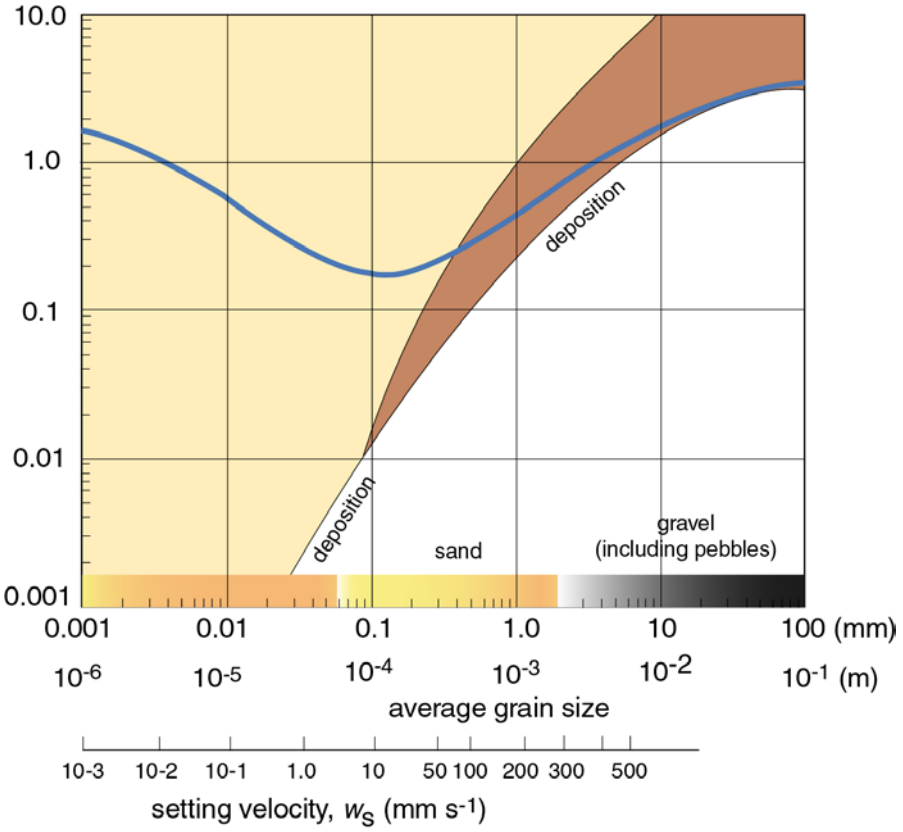

Figure 2.1 Illustrates the relationship between average particle sizes of sediments and the current speeds. (Modified after Wright et al. 2003)

2.4.2 Erosion

Natural causes of erosion are those, which occur as a result of the response of the beach to the effect of nature. Human induced erosion occurs when human endeavors impact on the natural system. Much of the human induced erosion is caused by negligence and lack of understanding and can be successfully avoided to certain extend.

Most of the erosion in the coastal zone is accomplished by waves.

Erosion proceeds through several processes:

- Mechanical impact of rushing water (and abrasive particles that it carries) against the shore.
- Pneumatic action - abrupt compression and expansion of air in rock crevasses as a wave breaks on the shore.
- Chemical action
  - Dissolution of rocks
  - Crystallization of salts in rock
- Erosion is most effective at the sea level or just above it, where wave erosion carves notches, which lead to undercutting and collapse of the whole slope.

Table 2.1: Natural and man-induced causes of erosion.

Natural	Man-induced
Sea level rise	Land subsidence from removal of subsurface resources.
Variability in sediment supply to the littoral zone	Interruption of material in transport
Storm waves	Reduction in sediment supply to the littoral zone
Wave and Surge overwash	Concentration of wave energy on the beaches
Deflation	Increase water level variation
Longshore sediment transport	Change natural coastal protection
Sorting of beach sediment	Removal of material from the beach

2.4.3 Coastal sediment transport

Shores erode, accrete, or remain stable, depending on the rates at which sediment is supplied to and removed from the shore. Littoral transport is a movement of sedimentary material in the littoral zone that extends from the shoreline to just beyond the seaward-most breakers.

Waves typically approach the shore at an angle (Figure 2.2-a). Swash moves sand diagonally, while backwash moves it straight down (Figure 2.2-b). The net result of this zigzag movement is the downwind displacement of sand

along the beach, known as beach drift. Besides the beach drift, longshore currents also transport sediments downwind - longshore drift. Together beach drift and longshore drift are called littoral drift (littoral is the zone between the lowest and the highest tides). Figure 2.2-c also shows how littoral drift leads to growth of sand *spit* across a bay.

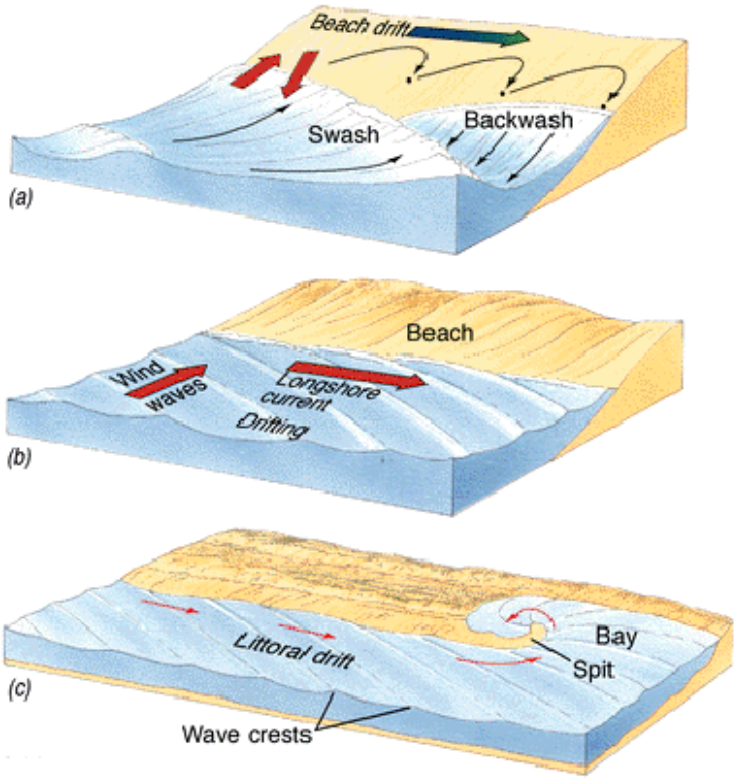

Figure 2.2. Describing longshore sediment transport (from the web).

Littoral drift = Beach drift + Longshore drift

Onshore-offshore transport has an average net direction perpendicular to the shore. Sediments are transported as:

a) Bed load transport
b) Suspended load transport
c) Wash load transport

The rate of sediment transport is the mass of sediment that is moved past a given point or through unit area of the water column in unit time. It is also called the sediment flux. The total of both bed load and suspended sediment flux is considered as total sediment transport rate.

a) Bed load transport

The bed load is the part of the total load that is more or less in contact with the bed during the transport. It primarily includes grains that roll, slide or bounce along the bed. Thus the bed load movement is governed by the shear velocity at the bed and effective resistance of the sediment particle. Although it is difficult to make predictions about bedload transport rate in marine environment, experiment and theory suggest that the rate of bedload transport (q_b) is proportional to the cube of the shear velocity, i.e.

$$q_b \propto u_*^3 \qquad \text{---------- } 2.1$$

provided that the shear stress at the bed is greater than critical shear stress. Since shear velocity is itself related to average current velocity the rate of bedload transport is also proportional to the cube of average current velocity measured at a fixed height above the bed. The equation 2.1 suggests that even very small changes in current speed or bed roughness can have significant effects on the rate of bedload transport.

b) Suspended load transport

The suspended load is the part of the total load that is moving in suspension without continuous contact with the bed as a result of agitation of fluid turbulence. Many estuary deposits contain large proportion of fine sediments, which are readily set in motion by tidal currents. The primary transport mode of fine sediments is in fact as suspended load and such sediment may amount to 75-95% of the total load in estuaries. The determination of the rate of suspended load transport is straightforward by comparison with measurement of the rate of bedload transport.

Current speed and sediment concentrations are measured throughout the water column and then suspended sediment flux, q_S is calculated by multiplying

the two. An Acoustic Doppler Current Profiler (ADCP) can measure both current speed and suspended sediment concentration from a vessel underway.

c) Wash load transport

The first two modes of transport, which together are called total load transport has effects on the bed morphology. The third mode of transport, wash load is not important as it consists of very fine particles transported in water and not represented in the bed.

2.4.4 Coastal deposition

Coastal erosion and deposition are very dynamic in nature. When the energy of waves changes, the balance between erosion and deposition also shifts. Normally, beaches grow during quiet weather and retreat (they are eroded) during storms. Only coarser sediment (grains larger than about 0.1-0.2 mm diameter) is transported as bedload. For a given grain size, these particles will stop moving when the bed shear stress is only a little less than the critical shear stress that was needed to start them moving. Particles in suspension will begin to settle towards the bed as soon as gravitational forces exceed buoyancy forces, but grains larger than about 0.1 mm will continue to move as part of the bedload, perhaps being taken intermittently back into suspension by eddies.

Particles smaller than about 0.1 mm do not go through a stage of bedload transport and are deposited directly from suspension. Moreover, as a current slows down, suspended particles of a given grain size do not all reach the bed at the same time because they will be distributed at different depths in the water column; and hence the rate at which suspended sediment is deposited depends on more than just the decrease in current speed. The time that particles take to settle will depend to a larger extent on their settling velocities and on the degree of turbulence in the water column - and while the particles are settling, they

continue to be transported in the direction of net current flow. Since very small particles settle significantly more slowly than large ones, they will eventually reach the bed some distance from where they began to settle, i.e. there is a settling lag. Also grains of slightly different size may settle at very different rates because settling velocities of small particles are proportional to the square of the diameter. So, for particles in the clay to very fine sand range, a very small decrease in grain size results in a significant change in settling velocity, and settling lag thus increases dramatically with decreasing particle size.

2.4.5 Littoral deposits

Sediments on most beaches range from fine sands to cobbles. The size and character of sediments and the slope of the beach are related to the forces that the beach is exposed to and the type of material available on the coast. When particles reach the shore as sand, they are moved alongshore by waves and currents. This longshore transport is a constant process, and great volumes may be transported. Beach material is also derived from erosion of the coastal formation caused by waves and currents, and in some cases, brought onshore by movement of sediment from deeper water. In some regions, a sizable fraction of the beach material is composed of marine shell fragments, coral reef fragments, and volcanic materials. Clay and silt do not usually settle on ocean beaches because the waves create such turbulence in the water along the shore that these fine particles are kept in suspension. The particles settle and deposit on the bottom only after moving away from the beaches into the quieter water of lagoons and estuaries or the deeper water offshore.

The mechanisms and descriptions of sediment transport are largely divided into two types: cohesive and non-cohesive. Cohesive sediments are characterized by cohesive/adhesive binding and by consolidation wherein attributes of the bulk sediment define the response of the grain. They usually comprise muddy sediments typical of estuaries, lakes, or the deep sea. Non-

cohesive sediments are characterized by their granular appearance (sand or gravels) wherein the attributes of the grain define the response of the bulk sediment.

2.5 Sediment transport measurements

Coastal engineers, physical oceanographers and geomorphologists generally carry out measurements of sediment transport using the following methods :

1	Wave refraction studies	Determines places of wave convergence or divergence and provide quantitative measurement
2	Using geomorphic indicators	Based on geomorphic indicators sediment transport direction is decided
3	Sedimentological methods	Beach profile study, sediment budget measurement.
4	Sediment trap study	Suspended sediments are collected in sediment trap and are measured
5	Artificial tracer tracking	Sediment transport direction detected from the movement of artificial tracers

Investigations such as sedimentological field studies, wave measurements or tracer tracking techniques are limited to small area coverage and are short-term studies. These studies are laborious, time consuming and uneconomic for covering long coastlines. Moreover, short-term studies of net sediment transport are prone to errors. Such investigations tried over a few months time only record seasonal changes and not long term changes i.e. net littoral drift. However, these studies are very useful to understand seasonal variability, rip currents and erosion-accretion patterns locally (Kunte et. al. 2001).

Computer-aided wave refraction studies determine places of wave convergence and divergence, rip currents and provide quantitative measurements of littoral drift and direction for local as well as regional areas. Such measurements are well trusted and used by coastal engineers. However,

the data are collected for short duration and hence no long-term drift evidences can be determined. Long term (for more than 100 years) data on wave energy, wave period, and wave height for specific beaches are not available. Additionally, drift determination based upon wave hind casting and the construction of wave orthogonal is subject to the vagaries of judgment and calculations of the investigators. Serious mistakes can be made by utilizing these methods without adequate verification of geomorphology and sedimentology of the coastal stretch under consideration (Kunte et al., 2002a)

Coastal landforms respond to all the variables of shore drift and record evidences during their course of formation and hence systematic study of these landforms provide reliable long-term littoral drift information. Hence such studies carried out with the help of remote sensing provide reliable results in short duration. Studies based on geomorphic indicators, determine littoral drift cells and drift direction within each cell and net littoral drift direction along the coast (Kunte et al., 2002a).

Shore drift is defined as the movement of beach material parallel to the coast in the near shore region caused by waves approaching the coast at an angle. It plays an important role in determining areas of coastal erosion and accretion, in shaping and orienting coastal landforms and finally in evolving the coast. Hence in the analysis of coastal erosion-accretion problems, for the development of harbor and construction of coastal structures, the direction, amount and behavior of long-term average shore drift is of vital importance.

2.5.1 Net Shore Drift Direction Determination

Net Shore Drift Direction (NSDD) is the direction in which sediments are transported along the shore over a period of year's in-spite of short-term

seasonal transport in the opposite direction. Net Shore drift directions may change from one coastal sector to the next due to the variations in coastal orientation and nearby oceanographic conditions. Each coastal segment with a particular net shore drift direction forms a discrete unit called a `drift cell' (Taggart and Schwartz, 1988). Each drift cell consists of three broad zones: a) zone of sediment supply or erosion, b) zone of transport, and c) zone of accumulation.

As net shore drift direction may results from all shore drift directions, it is necessary to understand shore drift within each drift cell. Since the shore drift is variable with respect to direction, time, place, duration and amount, the task of determining the net shore drift requires methods, which will take these variables into consideration.

2.5.2 Coastal landform indicators

Coastal landforms respond to all the variables of shore drift during their coarse of formation and hence these landforms can be considered as reliable long-term shore drift indicators. Their shape, size, form, pattern, development and their location, orientation and association with other landforms are important to study while determining net shore drift direction.

Several shore drift indicators are reported in literature (Table 2.2) Out of these, some indicators like stream mouth diversion, spit growth, beach width and man-made structures interrupting shore can be clearly mapped by remote sensing techniques.

Table 2.2 Indicators of shore drift direction.

Beach width	Increases in down drift direction

Sediment size gradation	Decrease in shore drift direction
Beach slope	Slope decreases in downdrift direction
Buff morphology	Bluff slope decreases in drift direction
Headland bay beaches	Grain-size and beach slope increases with increase in dist. from headlands.

Site Specific Indicator identifiable with Remote Sensing

Man-made structures interrupting shore drift	Accumulation of sediments on updrift side
Stream mouth diversions	Offsets in drift direction.
Inlet migrations	Migrate in drift direction
Spit growth	Grows in the direction of drift
Identifiable sediment	If source is known
Plan configuration of delta	Sediment accumulation in the up-drift side
Beach pads	Bar extends seawards from the beach pad in downdrift direction.
Near shore bars	Shore bar angle away from the shore in the direction of net shore-drift.
Beach location	Usually on updrift side.
Intertidal fans	Accumulation of sediments on updrift side
Recession of active cliff	Indicate change in orientation of shore lines
Paleo-beach ridges	Beach ridges indicate shore drift of past.

2.6 **Modeling approach** :

Sediment dynamics research in the past has relied heavily on theoretical, field, and laboratory analyses of the problem of sediment transport. These have proved inaccurate and often misleading as problem in nature is much more complex than hitherto considered due to complex bed evolution. There is a growing body of scientific literature indicating that the factors influencing sediment transport are strongly controlled by natural influences such as: sub-aerial exposure, water table fluctuations, hydrodynamic parameters, water and pore water chemistry, wave loading, and bed roughness amongst others. Consequently, there is a movement towards in-situ monitoring and modeling of sediment transport and the factors that influence it.

A better understanding is needed of the basic dynamics that control sedimentary processes such as bottom roughness, aggregation or flocculation and disaggregation, erosion and deposition, and bed consolidation. While the requisite observations and theoretical studies are beyond the scope of a modeling effort, a well tested community model would provide a valuable platform for testing and comparing emerging parameterizations of sedimentary processes. The ability to realistically simulate sediment transport is often limited by the ability to formulate laws for essential sediment processes from first principles, not by the efficiency and sophistication of our numerical models.

The following five sediment transport models are used of the many available models:

- EFDC, a freely-available, curvilinear orthogonal coordinate, coupled hydrodynamic, water-quality, and sediment model developed by TetraTech, Inc. and currently being improved by the U. S. Environmental Protection Agency.
- STP, the non-cohesive sediment transport program included in both the LITPACK (1D coastal processes) and MIKE 21 (2D wave, hydrographic and sediment transport processes in estuaries and coastal areas) packages marketed by the Danish Hydraulic Institute.
- CH3D-U.FI, a non-orthogonal curvilinear grid academic model developed under the leadership of Y. Peter Sheng at the Univ. of Florida.
- CH3D-ACOE, derived from an earlier version of the Univ. of Florida model and used for engineering studies by the U. S. Army Corps of Engineers.

- ECOM-SED, built around the Blumberg-Mellor hydrodynamic model and commercially marketed by HydroQual, Inc. and Delft Hydraulics.

---------- ---------- ----------

Chapter 3 – Digital Remote Sensing Data Processing

Chapter 3

DIGITAL REMOTE SENSING DATA PROCESSING

3.1 Introduction

Satellite remote sensing involves gathering information about features on the Earth's surface from orbiting satellites. These satellites carry two types of sensor systems known as "active" and "passive". A "passive" system generally consists of an array of small sensors or detectors that record (as digital numbers) the amount of electro-magnetic radiation reflected and/or emitted from the Earth's surface. A multispectral scanner is an example of a passive system. An "active" system propagates its own electro-magnetic radiation and measures (as digital numbers) the intensity of the return signal. Synthetic Aperture Radar (SAR) is an example of an active system. The digital data acquired by the satellites is transmitted to ground stations and can be used to reconstitute an image of the Earth's surface not too dissimilar to an aerial photograph.

Remotely sensed data acquired by the satellites have a number of distinct benefits for studying the Earth's surface, including:

- Continuous acquisition of data
- Regular revisit capabilities (resulting in up-to-date information)
- Broad regional coverage
- Good spectral resolution (including infra-red bands)
- Good spatial resolution
- Ability to manipulate/enhance digital data
- Ability to combine satellite digital data with other digital data
- Cost effective data
- Map-accurate data
- Possibility of stereo viewing

- Large archive of historical data

The word “Remote Sensing” is commonly used to describe the science of identifying, observing, and measuring an object without coming into direct contact with it. This process involves the detection and measurement of radiation of different wavelengths reflected or emitted from distant objects or materials, by which they are identified and categorized by class/type, substance, and spatial distribution.

The entire array of electromagnetic waves comprises the electromagnetic (EM) spectrum. The EM spectrum has been arbitrarily divided into regions or intervals to which descriptive names have been applied. At the very energetic (high frequency; short wavelength) end are gamma rays and x-rays. Radiation in the ultraviolet region extends from about 1 nanometer to about 0.36 micrometers. It is convenient to measure the mid-regions of the spectrum in these two units: micrometers (μm), or nanometers (nm). The visible region occupies the range between 0.4 and 0.7 μm, or its equivalents of 400 to 700 nm. The infrared (IR) region, spans between 0.7 and 100 μm. At shorter wavelengths (near 0.7 μm) infrared radiation can be detected by special film, while at longer wavelengths it is felt as heat.

The ability of the atmosphere to allow radiation to pass through it is referred to as its transmissivity, and varies with the wavelength/type of the radiation. The areas of the EM spectrum that are absorbed by atmospheric gases such as water vapor, carbon dioxide, and ozone are known as absorption bands. In Figure 3.1, absorption bands are represented by a low transmission value that is associated with a specific range of wavelengths. In contrast to the absorption bands, there are areas of the electromagnetic spectrum where the atmosphere is transparent (little or no absorption of radiation) to specific wavelengths. These

wavelength bands are known as atmospheric "windows" since they allow the radiation to easily pass through the atmosphere to Earth's surface.

Most remote sensing instruments on aircraft or space-based platforms operate in one or more of these windows by making their measurements with detectors tuned to specific frequencies (wavelengths) that pass through the atmosphere. When a remote sensing instrument has a line-of-sight with an object that is reflecting sunlight or emitting heat, the instrument collects and records the radiant energy. While most remote sensing systems are designed to collect reflected radiation, some sensors, especially those on meteorological satellites, directly measure absorption phenomena, such as those associated with carbon dioxide (CO_2) and other gases. The atmosphere is nearly opaque to EM radiation in part of the mid-IR and all of the far-IR regions. In the microwave region, by contrast, most of this radiation moves through unimpeded, so radar waves reach the surface. Weather radars are able to detect clouds and precipitation.

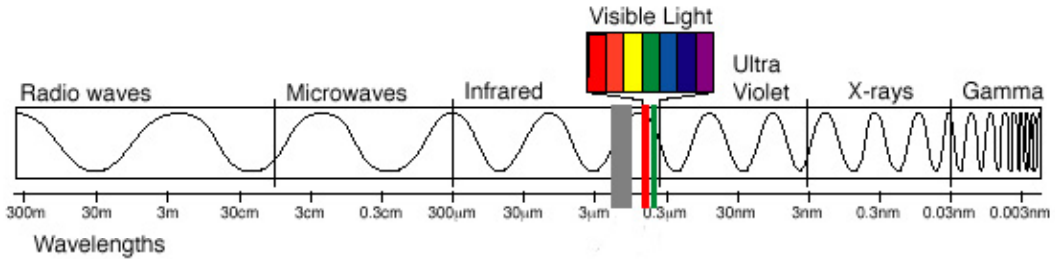

Figure 3.1. The Electromagnetic Spectrum

Satellite remote sensing provides an important and unique source of information for studies of earth system. There are currently over 45 missions operating, and over 70 more missions, carrying over 230 instruments, planned for operation during next 15 years by the world space agencies. The satellite remote sensing data are highly complementary to those collected by in-situ systems. The satellite data are often necessary for the provision of synoptic, wide-area information

required to put in-situ measurements in global context required for the observation of many environmental and climatic phenomena.

Present-day applications of satellite data are widespread and cover researches, operational and commercial activities. These activities are of interest in the global as well as regional, national and local context. A few major applications of satellite remote sensing data are listed below:

- Climate change research relies on operational and research systems to generate high-quality, consistent, global datasets for use in understanding the global climate system, validation of climate models and prediction of the impact of changes.
- Operational satellite measurements of surface, sea and upper air winds and atmospheric temperature fields provide major inputs to global weather forecasting.
- Agriculture and forestry services utilize satellite data to provide mapping information, crop health statistics, yield predictions and estimate rainfall amount.
- Resources (like water, mineral and forest) mapping utilizes high-resolution satellite data to map them even in inaccessible regions.
- Satellite data has been very useful in hazard monitoring and disaster assessment schemes.
- Ice movement monitoring with satellite data is provided as an operational service in many parts of world.
- Coastal zone management benefits largely from satellite information on parameters like water quality, suspended sediment and sea surface temperature.
- In oceanography, it provides accurate information on likely fishing grounds, ocean wave forecasting, measurement of sea floor topography and oil slick pollution monitoring.

There are two types Earth observation satellites, polar and geostationary. Polar-orbiting satellites typically operate at an altitude of around 800 km, with a revisit time of 2-3 days, whereas geostationary satellites operate in time scales of hours, which could theoretically provide data on the diurnal variation. The polar-orbiting sensors can be divided into two groups, dedicated polar orbiting sensors with a resolution greater than 500m, and hyperspectral sensors. At present, all operating, and most of the planned ocean-colour sensors are polar-orbiting satellites.

Polar orbiting satellites follow an overhead path around the Earth so that they pass close to the North and South Poles. They orbit the Earth as it turns beneath them. By so doing, a different part of the Earth's surface is viewed on each successive orbit. In this way the entire Earth is covered, with a small amount of overlap at low latitudes, and a greater overlap at higher altitudes. Satellite orbits can be controlled so that they view the same latitude on the Earth's surface at the same local sun time (referred to as *sun-synchronous*). The OCI sensor differs from other ocean-colour satellites, most of which are in sun-synchronous orbits, as it is to be placed at a 35º inclination with a 600 km circular orbit. Most ocean-colour sensors are on satellites at an altitude of around 700-800 km.

3.2 Ocean Remote Sensing

Space observations provide synoptic and repetitive coverage of the ocean in contrast to the sparse and isolated in-situ ship observations. Certain measurements specific to the orbital platforms such as sea surface height have been possible only through satellite oceanography. Despite the fact that measurements provided by sensors pertains to the sea surface only, they do manifest the dynamical oceanic processes beneath. To monitor key relevant ocean parameters, a wide range of different satellite systems and sensors is and will become available during

the decade. A detail account of remotely detectable oceanographic parameters and sensors is provided in Table 3.1. Polar orbiting satellites can monitor large-, regional-, and mesoscale weather and ocean features with sensors operating in a wide part of the electromagnetic wave spectrum whereas microwave sensors acquire data independent of sunlight and clouds. Understanding the importance of satellite observations in oceanography, a number of international cooperative scientific programs such as Global Ocean observation system (GOOS), World Ocean Circulation Experiment (WOCE), Joint Global Ocean Flux study (JGOFS) are in operation and are drawing open a variety of geophysical parameters.

Table 3.1. Remotely detectable oceanographic parameters and sensors.

Ocean parameter	**Payload/sensor**	**Area and time coverage**	**Remark**
Chlorophyll Concentration	Visible/infrared CZCS, SeaWiFS, OCM	Global, Once in 2 days	Narrow band, resolution 1km, swath 1500.
Sea Surface Temperature	Thermal infrared (TIR), (AVHRR, ATSR/UW, HIRS/MSU) scanning passive microwave Multi-channel Radiometer.	Global Daily	Split channel Better Resolution 1 km
Surface wind speed & direction	Scatterometer, (wind model), Passive microwave radiometers	Global Daily	Poor resolution, All weather Resolution 25 to 75 km.
Wave Height	Altimeter	Global 3 days	Resolution 10 cm in height measurements
Wave direction spectra	SAR	3 Days	SWH 0.5 m or 10%
Ocean currents, Sea surface topography	Altimeter	2 days	25 km.
Tides	Altimeter	2 days	----
Eddies/Gyers/Upwelling	TIR & Altimeter	2 days	TIR wide swath Altimeter –25 km

Internal waves	SAR & visible	3 days	20 m resolution
Ocean parameter	**Payload/sensor**	**Area and time coverage**	**Remark**
Bathymetry	SAR & visible	No critical, 20 m resolution	Only in shall waters
Sediments	Visible & near Infrared	----	For coastal waters only
Salinity	Airborne Lidar	---	Only at R&D level
Oil Slicks/pollution	SAR, Visible & infrared and thermal	Global	Large area detection
Sea and swell height/ direction/ period/wavelength	Altimeter, Scatterometer and SAR.	Global	---
Ocean Geoid	Altimeter	Global res- 25 km	For updating Geodatic data
Sea mounts	Altimeters	Global res- 25 km	Charting of deep sea
Heat budget	TIR & Scatterometer	Global	Derived from SST and Wind
Precipitation	SMMR, SSM/I	Daily Res – 1-10 km	Planed in TRMM
Cloud cover	INSAT, NOAA	1 km, 6 hrs.	AMSU/AIR
Humidity	METEOSAT	50 km , one day	AMSU profile.
Strom surge	Altimeter/scatterometer	25-50 km, Daily	---
Sea ice	SAR, MWR	20-25 Km, weekly	--
Coastal zone mapping	Visible, IRS, OCM	10 Km, 15 days	--
Mangroves	Visible & NIR	5-10 m, monthly	
Corals	Visible & NIR	5-10 m, monthly	
Coastal currents & Sea level	OCM, TIR, Altimeter	25 Km., 2 days	

In the present study of sediment transportation in the Gulf of Kachchh, ocean remote sensing is utilized for following three purposes.

1. For quantitatively assessing the suspended sediments by digitally analyzing Sea WiFS data using SEADAS software.
2. For detecting and monitoring movements of dispersed suspended sediment pattern within study area by image processing of ocean color monitor data.
3. For extracting sea surface temperature data from AVHRR/NOAA for model validation and wind parameters from Quiksat observations for inputting wind data to the model.

3.3 Ocean Color Remote Sensing

The need for information on spatial and temporal distribution as well as quantitative estimation of ocean water constituents such as phytoplankton and total suspended matter (organic & inorganic origin) has been long recognized in oceanographic studies. In continental shelf waters, an understanding of photosynthetic processes (primary production) is required to access the marine biological resources of the globe. Ocean color information on global scale is also of importance in studying the bio-geo-chemical cycles of carbon, nitrogen, and sulphur. The dispersion and transportation of inorganic suspended sediments are useful in the study of coastal processes. In the deep ocean, and in shallow sea, the ocean color features can be used as natural tracers to reveal transport processes. The pattern of color distribution, revealing streakiness and patchiness, contain spatial information about dispersion and mixing processes.

During passed three decades, the methods of detecting and mapping seawater constituents from aircraft and from space-borne platform have been successfully developed (Clarke, et al. 1970, Gordon and Morel, 1983; Evans and Gordon, 1994). Based on this experience, NASA launched the Coastal Zone Color Scanner (CZCS) sensor on

Nimbus – 7 in 1978 (Hovis et al, 1980). The CZCS demonstrate the feasibility of the measurements of phytoplankton pigments, and possibly even productivity (Morel A.1991, Platt et al. 1991) on global scale. The forerunner of all the ocean-color satellite sensors, the CZCS (1978-1986), has led to a series of sophisticated new generation of instruments such as MOS on IRS-P3, OCTS, POLDER, SeaWiFS, OCM on Indian Remote sensing Satellite P4, MODIS, MISR and OCI etc. A large number of ocean color payloads such as GLI, OSMI MERIS and PODDER-2 are awaiting launch in near future. The specifications of sensor on-board historic, current and scheduled satellites used in ocean color remote sensing are provided in table no 3.2.

Table 3.2. The specifications of sensor on-board historic, current and scheduled satellites used in Ocean Color remote sensing

Historic Satellite Ocean Color Sensors:

SENSOR	AGENCY	SATELLITE	OPERATING DATES	SWATH (km)	RESOL-UTION (m)	NUMBER OF BANDS	SPECTRAL COVERAGE(nm)
CZCS	NASA (USA)	Nimbus-7 (USA)	24/10/78-22/6/86	1556	825	6	433-12500
OCTS	NASDA (Japan)	ADEOS (Japan)	17/8/96 – 1/7/97	1400	700	12	402-12500
POLDER	CNES (France)	ADEOS (Japan)	17/8/96 - 1/7/1997	2400	6 km	9	443-910

Current Satellite Ocean Color Sensors:

SENSOR	AGENCY	SATELLITE	OPERATING DATES	SWATH (km)	RESOL-UTION (m)	NUMBER OF BANDS	SPECTRAL COVERAGE(nm)
MOS	DLR (Germany)	IRS P3 (India)	Launched 21/3/96	200	500	18	408-1600
SeaWiFS	NASA (USA)	OrbView-2 (USA)	Launched 1/8/97	2806	1100	8	402-885
OCI	NEC (Japan)	ROCSAT-1 (Taiwan)	Launched (Jan 1999)	690	825	6	433-12500
OCM	ISRO (India)	IRS-P4 (India)	Launched (26/5/1999)	1420	350	8	402-885
MODIS	NASA (USA)	Terra (USA)	Launched 18/12/1999	2330	1000	36	405-14385
MISR	NASA (USA)	Terra (USA)	Launched 18/12/1999	360	250	4	446-867
OSMI	KARI (Korea)	KOMPSAT (Korea)	Launched 20/12/1999	800	850	6	400-900

MERIS	ESA (Europe)	ENVISAT-1 (Europe)	Launched 01/03/2002	1150	300/1200	15	412-1050
MODIS-Aqua	NASA (USA)	Aqua (EOS-PM1)	Launched 04/05/2002	2330	1000	36	405-14385
OCTS China	CNSA (China)	HaiYang-1 (China)	Launched 15/05/2002	1400	1100	10	402-12500

Scheduled Satellite Ocean Color Sensors:

SENSOR	AGENCY	SATELLITE	OPERATING DATES	SWATH (km)	RESOL-UTION (m)	NUMBER OF BANDS	SPECTRAL COVERAGE (nm)
GLI	NASDA (Japan)	ADEOS-II (Japan)	Scheduled (Nov. 2002)	1600	250/1000	36	375-12500
POLDER-2	CNES (France)	ADEOS-II (Japan)	Scheduled (Nov. 2002)	2400	6000	9	443-910
S-GLI	NASDA (Japan)	ADEOS-3 (Japan)	Scheduled (2007)	1600	750	11	412-865
VIIRS	U.S. Gov. (USA)	NPP (USA)	Scheduled (2005)	1700	742	19	402-11800

The main objective of the ocean color remote sensing is the quantitative assessment of the oceanic constituents (e.g. chlorophyll, suspended particulate matter, yellow substances, etc) from the spectral nature of the solar radiation backscattered from the ocean waters. A bipartite classification scheme, according to which oceanic waters are partitioned into Case 1 or Case 2 waters, was introduced by Morel and Prieur (1977), and refined later by Gordon and Morel (1983) and Sathyendranath and Morel (1983). By definition, Case 1 waters are those waters in which phytoplankton (with their accompanying and covering retinue of material of biological origin) are the principal agents responsible for variations in optical properties of water. On the other hand, Case 2 waters are influenced not just by phytoplankton and related particles, but also by other substances that vary independently of phytoplankton, notably inorganic particles in suspension and yellow substances.

In case 2 waters, all inorganic particulate material that is not included in the phytoplankton component are included. In shallow and

inland water bodies, wave and current impacts can bring bottom sediments into suspension, modifying significantly the color of the oceans. It is important to recognize that the term suspended material does not apply to a single type of material, but a whole family of material with their own individual characteristics. Case 2 water may also include suspended particles of other origin, such as continental dust deposited on the water or volcanic deposits. In addition, light reflected from the bottom of a water body can also influence ocean color provided the water is sufficiently shallow and clear. Influence of bottom on the color of water can vary with the depth of water body, the clarity of the water, the type of substances present in the water, and type of bottom. The geographic distribution of Case 2 waters is variable: water of the given locality may drift between Case 1 and Case 2 conditions, depending upon environmental forcing.

The color of the water is determined by scattering and absorption of visible light by pure water itself, as well as the inorganic and organic, particulate and dissolved, material resent in the water. It is recognized that these substances vary independently of each other in Case 2 waters.

Out of solar radiation falling on the earth surface, only the visible portion of the spectrum can penetrate into water. This radiation, after entering into the sea water, undergoes absorption and multiple scattering by water molecules and the water constituents and a small part of it is scattered out which is detected by the ocean color sensor. The ocean-detected radiance is a mixture of radiation emerging from water (called water leaving radiance) and the solar radiation backscattering by the air molecules (Rayleigh scattering) and the aerosols (mainly Mie scattering) in the atmosphere. This part of radiation, called the atmospheric path radiance, is quite strong and constitutes more than 85% of the radiance at the Top of the Atmosphere (TOA). Therefore, to estimate the oceanic

constituent correctly, it is absolutely necessary to remove the atmospheric contribution from the detected radiances.

In order to carry out atmospheric correction, all the ocean color sensors are equipped with a few additional channels with wave lengths greater than 700 nm in which ocean surface will act as dark background due to high infrared absorption by water (Table 3.3).

Table 3.3. Ocean color sensors and their specific properties.

Sensor Parameter	SeaWiFS	MODIS	OCTS	OCM	GLI
GIFOV (Km.)	1.1 LAC 4.5 GAC	1.0	0.70	0.36	1.0
Swath (Km)	2801 LAC 1502 GAC	1780	1400	1420	1600
Repetivity (days)	2	2	2	2	2
Local Time (hr)	12 noon	13:30	--	12 noon	--
Scan Plane Tilt	+_20	+_50	+-20	+-20	----
Spectral	402-422	430-440	402-422	402-422	16bands
	433-453	485-495	433-453	433-453	
	480-500	515-525	480-500	480-500	
	500-520	560-570	500-520	500-520	
	545-565	615-625	545-565	545-565	
	660-680	660-670	660-680	660-680	
	745-785	680-690	745-785	745-785	
	845-885	760-770	845-885	845-885	
		+3 NIR & TR bands	3550-3880 8250-8800		
			10300-11400		
			11400-12500		
Quatz (Bits)	10	12	10	12	12
Absolute Radiometric AC	5%	<2%	<10%	<10%	--
Polarisation Sensitivity	<2%	<2%	<2-5%	<2%	--

In these wavelengths, all the detected radiances are due to scattering in the atmosphere and can safely assume to be zero. The Rayleigh scattering Lr is computed using well-established theory.

$$Lt = Lr + La + Lw$$

Once Lr is known then Lt is assume to be equal to La, i.e. the aerosol path radiance. A relationship has been obtained from the spectral behavior of the aerosol optical depth using channel 765nm and 865 nm. An exponential relationship for spectral behavior of aerosol optical depth has been used in the atmospheric correction algorithm. The aerosol optical thickness has been extrapolated to visible channels using this exponential relationship. From the radiances measured in the long wavelengths, the atmospheric path radiances in the ocean color wavelength are determined and removed from the sensor radiances through an atmospheric correction procedure. The water leaving radiance obtained after removing the atmospheric path radiances are subsequently utilized for the estimation of oceanic constituents using suitable biogeochemical algorithms.

3.4 Quantitative assessment using SeaWiFS data

Water is classified as case 1 (correlated) or case 2 (not correlated), depending on whether these concentrations are correlated among themselves. Coastal waters are often referred as case 2 water. In reality, even in coastal water phytoplankton, suspended sediments, and yellow substances are generally correlated, but correlation may exhibit large spatial and temporal variations as a result of local phenomena such as river drainage, bottom resuspension, and urban and industrial effluents. Until now only remote-sensing data relative to case 1 water have been routinely interpreted, yielding concentrations of phytoplankton pigments and to some extend suspended sediments. Almost no information was obtained on yellow substance contents.

A large number of algorithms have been proposed to quantify total suspended matter in the coastal sea (e.g. Klemas et al.1974, Tassan and strum 1986, Chauhan et al. 1996 etc.). Ruddick at el. (1998) used AVHRR for the determination of suspended particulate matter distribution and dynamics in the Belgian coastal waters. He used an analytical model of ocean color to provide a basis for optimal calibration of the relationship between AVHRR-derived reflectance and SPM concentration and to estimate the error introduced by independently-varying chlorophyll concentration. They found common features as a turbidity maximum offshore of Oostende and at the mouth of the Scheldt Estuary; can be found in both AVHRR reflectance imagery and in-situ measurements of SPM providing stropping evidence that SPM can be detected from AVHRR in this region.

Using an analytical model based on the difference of the NOAA/AVHRR Channel 1 and channel 2 reflectance data, Li et al. (1998) developed an algorithm for the retrieval of suspended sediment in the coastal and shelf waters. The formula is governed by the optical parameters of water and suspended sediments, including volume scattering and absorption coefficient of the two channels. They tested algorithm using data from seven transects in the China Sea, and the retrieved results for the Zhujiang Estuary were compared with the sea-truth data with good agreement.

Ruddick et al. (2000) attributed the failure of standard algorithm over turbid waters to invalid assumption of zero water-leaving radiance for the near-infrared bands at 765 and 865 nm. In there study they replaced these by assumptions of spatial homogeneity of the 765:865 ratios for aerosol reflectance and for water-leaving reflectance. The new algorithm performed satisfactory for imagery of Belgian coastal waters and yielded physically realistic water-leaving radiance spectra.

Kunte et al. (2002b) processed several Sea WiFS cloud-free images between October 1998 and August 2001 using standard algorithms from SeaDAS software for extracting chlorophyll concentration distribution. Principal component images generated from Ocean Color Monitor data collected on-board Indian Remote sensing Satellite were utilized to study turbidity distribution and dispersion pattern.

In this study, a three-component model, put forward by Tassan (1994), was applied to case 2 waters of the Gulf of Kachchh. A large set of reflectance values were simulated by independently varying concentrations of phytoplankton, suspended particulate matter, and yellow substances over the ranges generally encountered in the coastal zone. The water composition was then retrieved by principal component analysis. Sufficient orthogonality was noticed among the spectral signatures of the three main types of water constituents to permit their retrieval from the reflectance spectra. The reduction from full spectral data to 5 selected wavelengths did not cause any appreciable loss of retrieval efficiency. It was considered worthwhile to employ a similar computational scheme, which uses SeaWiFS data for retrieval of phytoplankton, sediment concentration as well as yellow substances in coastal water.

Tassan (1994) suggested following methodology for the Chlorophyll concentration ranging between 0.025-1.0 mg m^{-3}

For retrieval of C, the first choice was: $Xc = [R(\lambda_l)/R(\lambda_j)]\,[R(\lambda_m)/R(\lambda_n)]^a$

Where first factor λ_l, λ_j close to C absorption maxima and minima.
Second factors λ_m, λ_n are on either sides of absorption peak
So low dependence on C and high on S and A.
$R(\lambda)$ is reflectance value for certain wave length.

The final form of optimization routine was

$$Xc = [R(\lambda_2)/R(\lambda_5)]\,[R(\lambda_1)/R(\lambda_3)]^{-1.2}$$

Similarly for suspended sediments,

$$Xs = [R(\lambda_l)/R(\lambda_j)]\,[R(\lambda_m)/R(\lambda_n)]^{b}$$

And actual was

$$Xs = [R(\lambda_5)/R(\lambda_6)]\,[R(\lambda_3)/R(\lambda_5)]^{-0.5}$$

And for Yellow substance

$$Xy = [R(\lambda_1)/R(\lambda_3)]\,[R(\lambda_2)]^{0.5}$$

For Chlorophyll concentration ranging between 0.1- 40 mg m^{-3}

The final form of optimization routine for C was

$$Xc = [R(\lambda_2)/R(\lambda_5)]\,[R(\lambda_1)/R(\lambda_3)]^{-0.5}$$

Similarly for suspended sediments,

$$Xs = [R(\lambda_l)/R(\lambda_j)]\,[R(\lambda_m)/R(\lambda_n)]^{b}$$

And actual was

$$Xs = [R(\lambda_5)/R(\lambda_6)]\,[R(\lambda_3)/R(\lambda_5)]^{-1.2}$$

And for Yellow substance

$$Xy = [R(\lambda_1)/R(\lambda_3)]\,[R(\lambda_2)]^{0.25}$$

Least-squares fitting of the data computed for $\partial = 1$ yielded

$\log(c) = 0.36 - 4.38 \log(Xc)$, $1 < C(\text{mg m}^{-3}) < 40$

$\log(S) = 1.82 + 1.23 \log(Xs)$,

$$0.56 < S\ (\text{g m}^{-3}) < 4.6$$

This theory and algorithm proposed by Tassan is used to quantify suspended sediments using SeaWiFS data and Seadas algorithms. The SeaWiFS data for about 651 dates between October 1998 and August 2001 period, pertaining to the West Coast of India were browsed using available browsing facility at GSFC data center. Only 151 cloud-free or less clouded images were selected. Full resolution (1km) SeaWiFS data

for 151 cloud-free images were processed using Sun Solaris System and SEADAS 4.2 software. Water leaving radiance in bands 490, 555, and 670 nm were separated and used to compute suspended sediment by writing a script (program) based on following equations.

$$\text{Log } S = 1.83 + 1.26 \text{ Log } X_s \text{ ---- for } 0.0 \text{ </= } 100.0 \text{ mg/l S}$$

X is suspended sediments concentration in mg/l and Xs is variable defined as

$$X_s = [R_{rs}(555) + R_{rs}(670)]^* [R_{rs}(490) / R_{rs}(555)]^{-0.5}$$

Seadas software provides 24 flags. These flags provide much of diagnostic information useful in interpreting the images. Using the above-mentioned algorithm, several data sets pertaining to GoK were analyzed and results of 5 images for the December month are presented in Figure 3.2. Sediment distribution and dispersion is studied from plume patterns. Figure and color-code bar provides quantifications.

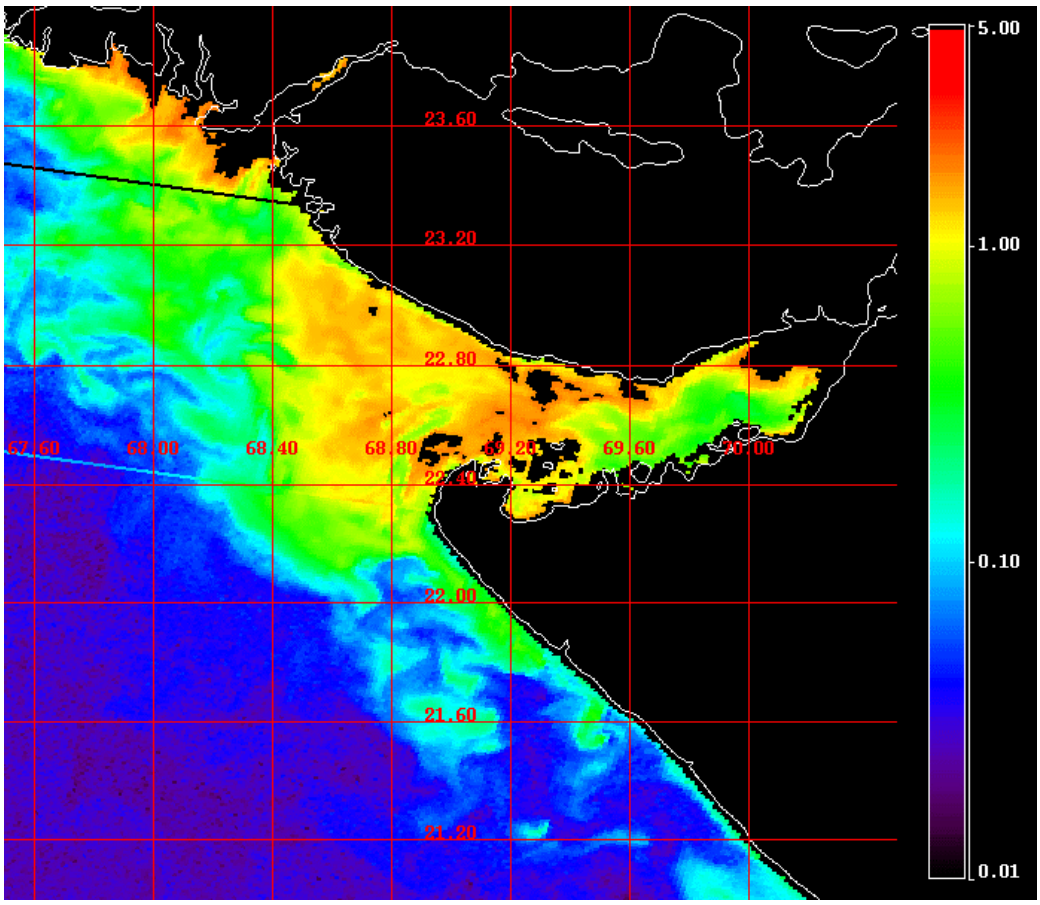

a) Data observed on 20th Dec 1999 at 07:46

Figure 3.2a. Suspended sediment plumes in Gulf of Kachchh derived from Sea WiFS data.

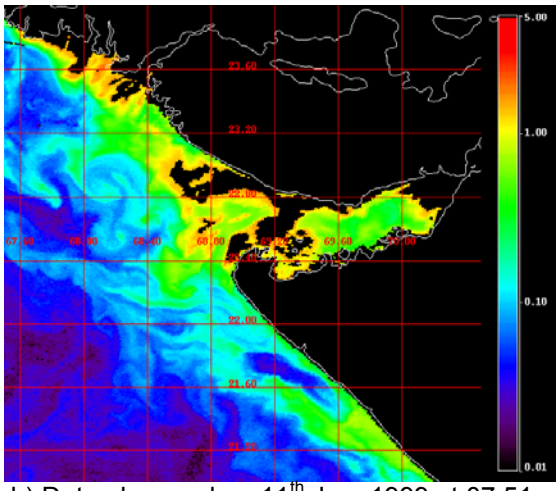

b) Data observed on 11th Jan. 1999 at 07:51

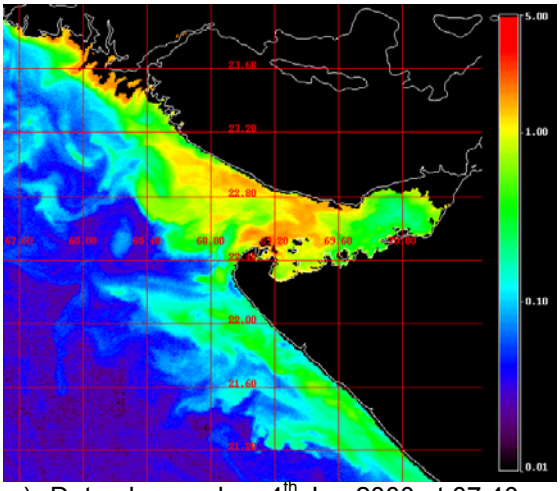

c) Data observed on 4th Jan 2000 at 07:40

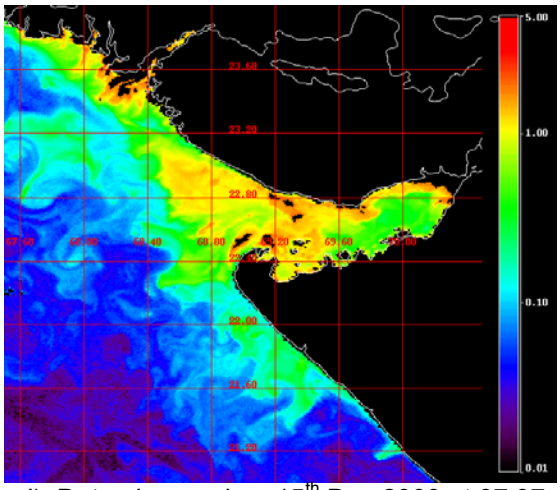

d) Data observed on 15th Dec 2000 at 07:37

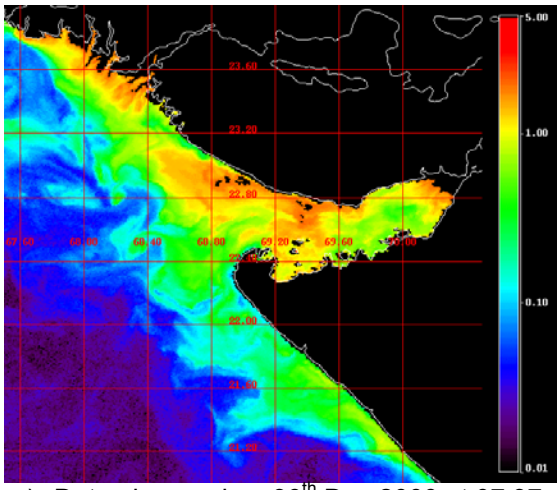

e) Data observed on 30th Dec 2000 at 07:37

Figure 3.2. Suspended sediment plumes in Gulf of Kachchh derived from Sea WiFS data.

3.5 Monitoring sediment patterns from OCM images

Analysis and interpretation of the satellite data using image processing techniques can help in monitoring patterns of suspended sediment movements. In the present study, image (video) data collected onboard Ocean Color Monitor (OCM) is utilized for understanding suspended sediment movements and for quantitative assessment.

The OCM is a solid-state camera, onboard Indian Remote Sensing Satellite (IRS P4). It provides resolution of 360 m in 8 VNIR bands (table 3.3) covering a swath of about 1500 km, every alternate day. OCM data (Path 9, Row 13, dated 2nd Jan 2000, and time 07:23:43, during mean tide) were digitally analyzed using an image processing system to generate a false color composite image, OCM FCC, with bands 5, 6 & 7 (RGB) (Figure 3.3).

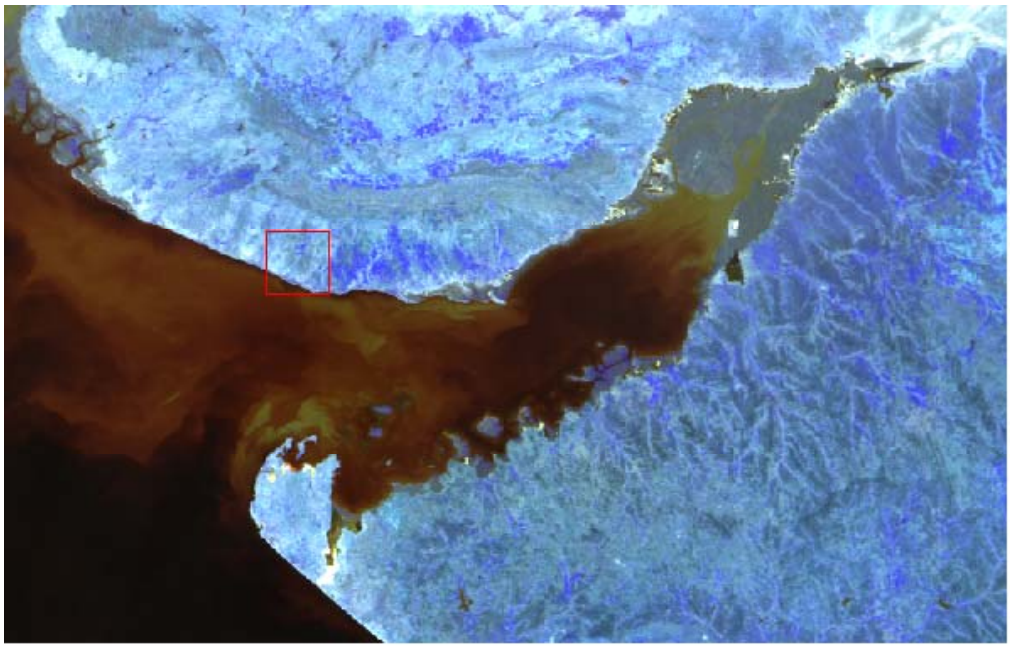

Figure 3.3 False colour composite of 5(B), 6(G), 7(R) bands of Ocean Color Monitor of Gulf of Kachchh (FCC1)

Principal component analysis was performed, as described in Kunte (1994), to achieve overall enhancement by selecting the best information from raw data and to reduce the dimension of data without much loss of information. Out of the eight principal components (Figure 3.4), first four components that contain approximately 95% of information, were used for interpretation. Two false color composites were produced from principal components (PCs) 2, 3 & 4 (RGB) and 1, 2 & 3 (RGB) (Figure 3.5 a, b). These enhanced images were enlarged to locate and decipher various coastal geomorphic units and underwater bed flow structures. Particular attention was paid towards mapping of sediment plumes to understand the distribution and dispersion of suspended and settled sediments (Figure 3.3). Available maps from earlier studies, topographic maps (41 F & J) and navigation charts (NHC-203) were used as base maps for reference. Geomorphic units, distribution and directions of suspended sediments, and current directions are marked on the OCM PC image (Figure 3.5a).

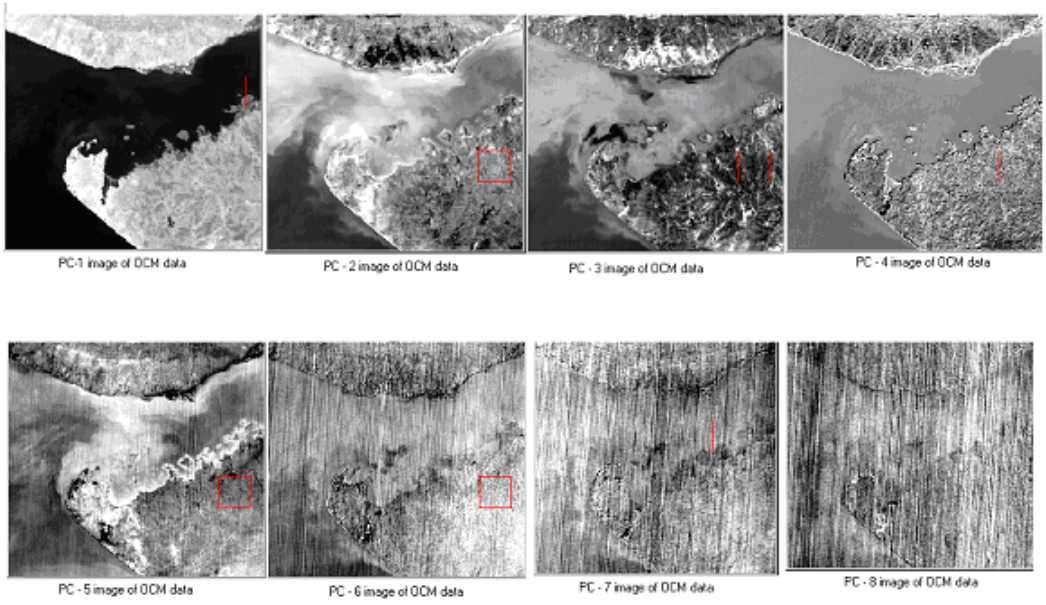

Figure 3.4 Principal Component Images generated from Principal component analysis of OCM data.

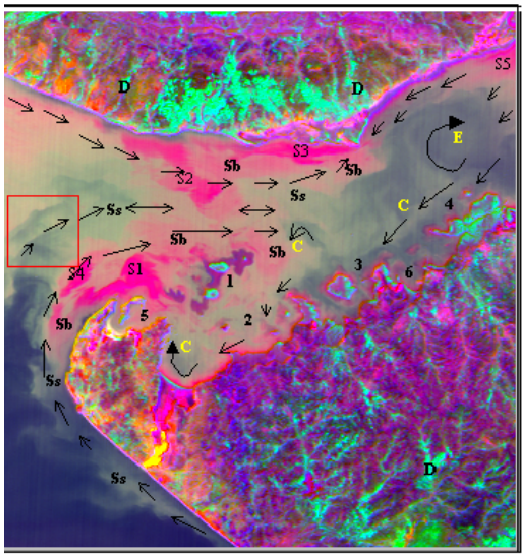

Principal Components 2-3-4 bands of OCM are displayed with Red-Green- Blue colors respectively.

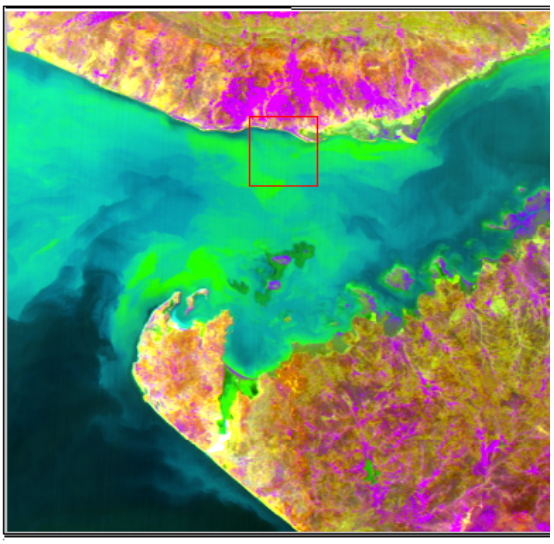

Principal Components 1-2-3 bands of OCM are displayed with Red-Green- Blue colors respectively.

Figure 3.5a (FCC2) and 3.5b (FCC3) (after Kunte et al. 2003)

Orbital images provide a synoptic view of submerged as well as discrete turbid water masses (suspended sediments) in the coastal waters of the gulf. Depending on the type of particulate matter, stratification, depth of settling and bottom condition, overlying water reflectivity changes in different shades of color. On the satellite images, the sharp contrast between various sediment-laden waters is clear and mappable. Tonal/color variation is considered as a measure of sediment concentration. Texture and pattern help in monitoring distribution and dispersion of sediment masses. On the satellite images, the sediment-laden plume indicates the current directions as they become elongated and pointed towards flow. Using these basic principles, all the three FCCs, and individual principal component images were studied. All enhanced satellite images were visually analyzed based on location, image characteristics and other associated features, and the geomorphic features within gulf and shore were finally marked on FCC-2 image (Figure 3.5 a) by assigning letters and direction arrows.

The first Principal Component (PC1) image display maximum variance contained in the original 8 bands and so from this image, boundaries of major geomorphic features like islands, creeks, spits etc are delineated (Figure 3.4). The PC2 image mainly highlights dispersion and distribution of suspended sediments. The PC3 image is exhibiting bed load features, current movement, islands, mangroves etc. In PC4 image, coastal geomorphic features are seen highlighted due to apparent relief whereas features in the gulf are subdued. PC 5, 6, 7, & 8 could not be used as principal component analysis generated these images with substantial noise.

The false color composite image, FCC-1 was prepared from spectral bands, 5(red), 6(green) & 7(blue) (Figure 3.3). FCC-2 was generated from principal components 2(red), 3(green), & 4(blue) (Figure 3.5a) whereas FCC-3 was produced from principal components 1(red), 2(green) & 3(blue) (Figure 3.5b). FCC –1 covers the entire Gulf of Kachchh and adjacent regions. The Gulf water and coastal boundary are noticeably highlighted due to color contrast. However other features like islands, spits, beaches, mangroves, shore drainage etc. are visible but are not readily recognized due to faint color shades. Mud flats in gray color, located at the head of the gulf are distinct in the image. Formation of mud flats at the Gulf head has blocked the entrance of one of the major source of fresh water. Suspended sediment plumes are seen emerging from these mud flats and migrating towards center of the gulf. Turbidity is greater towards the coast than in the middle.

FCC 2 and 3 (Figure 3.5a,b) display various image features in different bright colors and observable shades and contrast. While interpreting, both the images were simultaneously used. However, for describing various features, letters, numbers and arrows are marked and

are described as they appear on FCC-2. By comparing FCC-2 & 3, features are clearly recognizable on FCC-3, which appear in various colors and shades.

The northern shoreline is bordered mainly by sand (pink), mud (bluish), eastward growing spits (north-central shore), mangroves swamps, raised tidal flats etc. and is in-fronted by numerous shoals. Several drainage lines (in light greenish shades) are joining northern coast but show no sign of river plumes. Low-level coastal plains with indentations, deep inlets, near shore islands, reefs, mangrove swamps, mud, etc. mark the southern shore. On FCC 2, the island groups, as denoted by numbers 1-6, are partially covered by mud (violet) and remaining by mangrove swamps (sky blue). Most of the islands are surrounded by coral reefs (reddish violet). The reefs are in the form of fringing reefs, platform reefs, patch reefs and coral pinnacles. The shapes, sizes and locations of these islands, reefs, and mangrove swamps match well with those on topographic and navigational maps.

Within the Gulf, the most conspicuous features on the image are shallow submerged shoals (< 5 m water depth), deep submerged shoals (> 5 and <20 m water depth), suspended sediment plumes etc. Large pink colored irregularly shaped features are recognized as stable shallow submerged shoals after comparing with topographic contour on navigational chart. The large semicircular submerged shoal (Bobby shoal) denoted by S1, the Gurur Shoal (S4) are located at the entrance of Gulf near Okha. Both the shoals are elongated and pointed along the current direction. The mouth of the Gulf is also obstructed by Lushington shoal and, at the entrance on the northern coast, by the Ranwara shoals (S2). A large east-west trending shoal (S3) is located near northern shore. Kala Dhara shoal (S5) is located in the northeast corner of the image. The size, shape, and location of these shoals also match very well with those

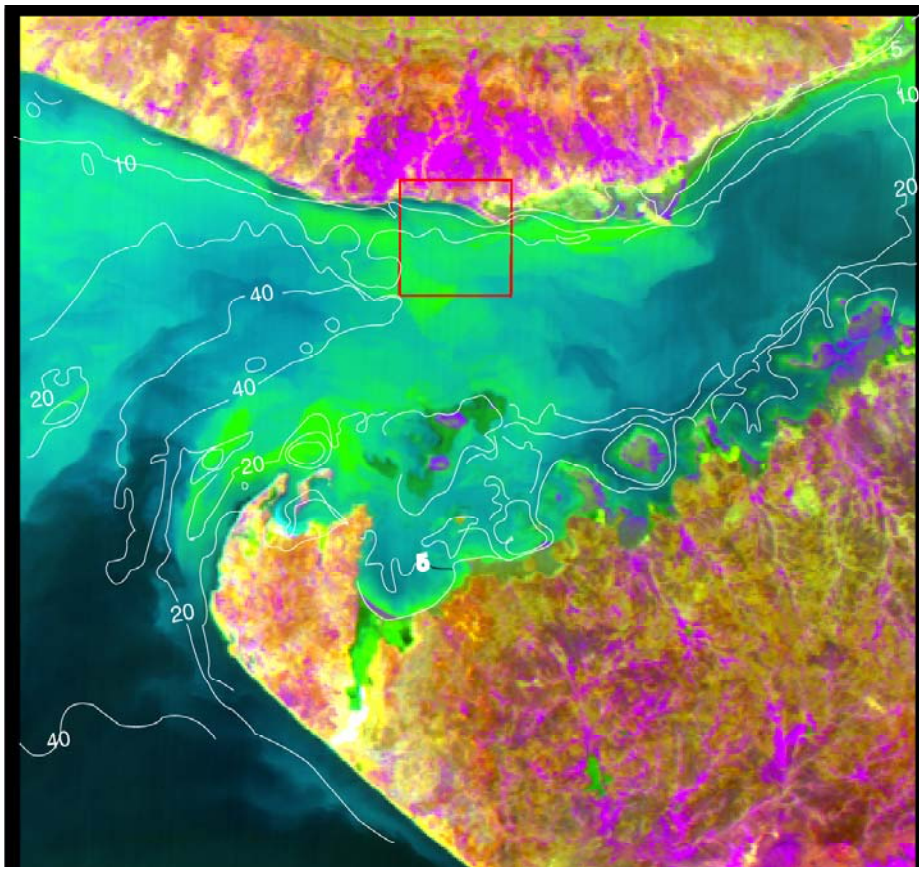

Figure 3.7 Principal Components 1-2-3 bands of OCM are displayed with Red-Green-Blue colors respectively. Bathymetry contours are superimposed (after Kunte at el. 2003).

marked on the Navigational charts. Depth of formation of Bobby, Ranwara, Gurur, and Lushington shallow submerged shoals correspond well with depths nearly 5 m below chart datum. Most of these shallow submerged shoals are surrounded by deep submerged shoals (light pink) as denoted by “Sb”. These shoals correspond to the depths between 5 and 20 m below water level. The largest of the submerged shoals is located to the northwest side and is visible even though lying at the depth of approximately 20 m.

Suspended sediments (in buff color denoted by Ss) are seen in dispersed pattern or as sediment plumes. Along the southeastern side of the southern shore, sediment plumes are seen approaching northwards.

Further northwards, majority of the plumes are entering the Gulf near Okha. From the northwestern side, dispersed sediment plumes, pointing southeastward are entering the Gulf. The direction of sediment movement is inferred as plumes elongate and point in the direction of movement. Due to the presence of shoals the suspended sediments are seen to be dispersed in the central part of Gulf. Deep water is indicated by deep blue color located to the southwestern side and in the central and eastern part of gulf. The area marked by a red square shows progressive gradation from light pink-buff-yellowish blue-blue indicating variation in sediment contained (Kunte et al. 2003).

Depending on the direction of elongation of submerged shoals and sediment plumes, the direction of tidal currents is inferred. At the locations denoted by 'Cs' clockwise, anticlockwise or curly movements of sediment indicate the current direction. A clockwise eddy structure is located at 'E'.

3.6 Sea Surface Temperature extraction from AVHRR/NOAA

The distribution of SST provides significant information related to a wide range of marine processes and phenomena such as ocean currents, fronts, mesoscale eddies, and up-welling phenomena. This allows use of satellite derived SST information in mapping of the ocean circulation, fisheries, algal blooms and in assimilation of SST data in dynamical circulation models. SST is observed from space by thermal infrared imagery, during cloud-free conditions, using the thermal infrared channels of the NOAA/AVHRR and from the ERS ATSR sensor systems. These instruments measure the SST distribution at a spatial resolution of 1 km and an accuracy of 0.5°C or better (NOAA, 1995).

Infrared radiance measurements have been used since 1970 to estimate sea surface temperature from space. The techniques for estimating sea surface temperature are based on the physics of blackbody

radiation. Solutions are also required to practical problems such as correcting for the effects of the intervening atmosphere, identifying cloud-free regions, and navigating the measurements to ground coordinates. The National Oceanic and Atmospheric Administration (NOAA) currently use two polar-orbiting satellites, NOAA-12 and NOAA-14, for twice-daily global observations of sea surface temperature. These satellites are equipped with the Advanced Very High Resolution Radiometer (AVHRR), which scans the surface with a nadir resolution of 1.1 km and continuously broadcasts the data to ground receiving stations within the line of sight.

Table 3.4 showing a listing of AVHRR wavelength channels.

Channel	Region	Wavelengths
1	Visible	0.58-0.68 μm
2	Reflected Infrared	0.725-1.1 μm
3	Emitted Infrared Window Channel	3.55-3.93 μm
4	Emitted Infrared Window Channel	10.33-1.3 μm
5	Emitted Infrared Window Channel	11.5-12.5 μm

Channels 1 and 2 measure reflected light in the visible and near infrared regions, respectively. Channels 3, 4, and 5 are dominated by radiation emitted from surface. Channel 3 has the advantage that it is less sensitive to atmospheric water vapor. However, channel 3 will admit a substantial amount of reflected solar radiation. It is, therefore, primarily used at night. Channels 4 and 5 are more affected by water vapor, but are not substantially contaminated by reflected solar radiation. It is the judicious combination of radiance measurements from channels 3, 4 and 5 that permits extraction of sea surface temperature.

Sea Surface Temperature Algorithms

Equations used to calculate Sea Surface Temperature from AVHRR Data

SST Equations for NOAA-12, -14, and -15 are as follows :

Night (split)

Ts = a0 + a1*band4 + a2(band4 - band5) + a3(band4- band5) (sec(theta) - 1)

Night (dual):
Ts = a0 + a1*band4 + a2(band3 - band4) + a3(sec(theta) - 1)

Night (triple):
Ts = a0 + a1*band4 + a2(band3 - band5) + a3(sec(theta) - 1)

Day (split):
Ts = a0 + a1*band4 + a2(band4 - band5) + a3(band4 - band5)(sec (theta) - 1)

Where Sec (theta) is the secant of the satellite zenith angle, and band 3, band 4, and band 5 are the calibrated brightness temperatures of AVHRR/NOAA bands (in Kelvin). The "a" coefficients used in the above equations are derived from a regression model based on global drifting buoy and tropical Pacific fixed buoy data. The coefficient values depend on which NOAA satellite was used to collect the AVHRR image.

Using the above method, sea surface temperatures for five different days in December and six days in November were derived after processing AVHRR/NOAA images (Figure 3.8 and 3.9). In the month of December, sea surface temperature is ranging between 22^0 and 27^0 C. It is observed that during all days temperature reduces from mouth of the Gulf towards head of the Gulf. Lower temperature is observed along southern boundary than northern boundary. Sea Surface Temperature observed using AVHRR/NOAA is found to be comparable with that of model results.

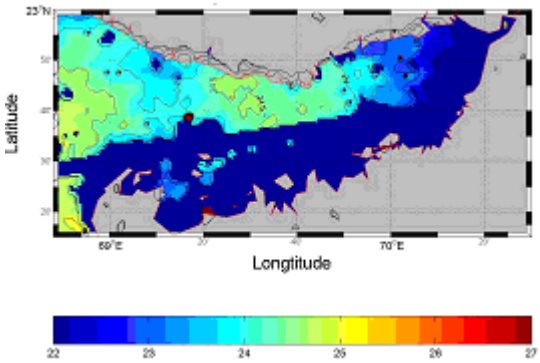

Date: 17-Dec-1999 Time:10:59 hrs

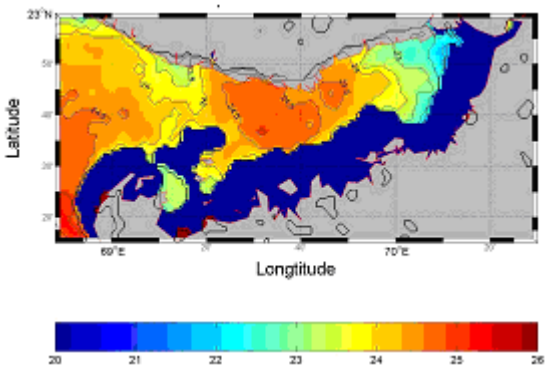

Date: 16-Dec-1999 Time: 11:10 hrs.

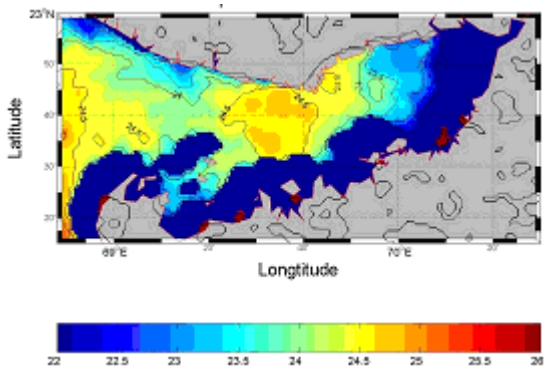

Date 15-Dec-1999 Time: 11:22 hrs

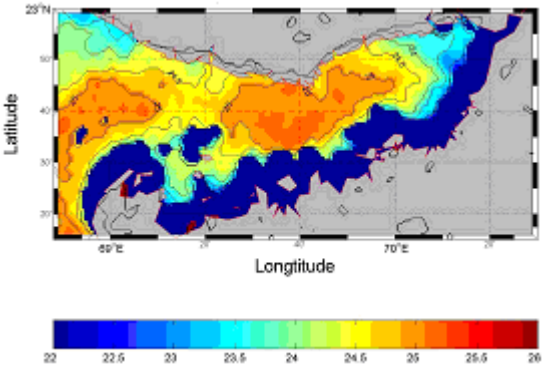

Date: 08-Dec-1999 Time: 11:01 hrs

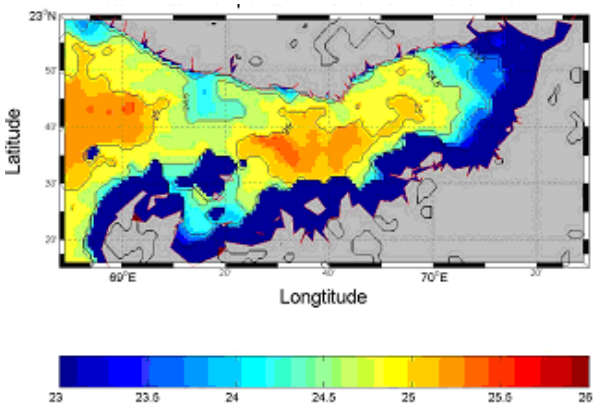

Date: 07-Dec-1999 Time: 11:12 hrs.

Figure. 3.8 Sea surface temperature measured by NOAA/AVHRR for 5 days of December-99

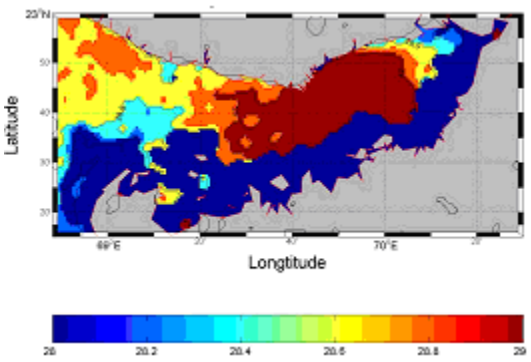

Date:02-Nov-1999 Time: 10:57 hrs

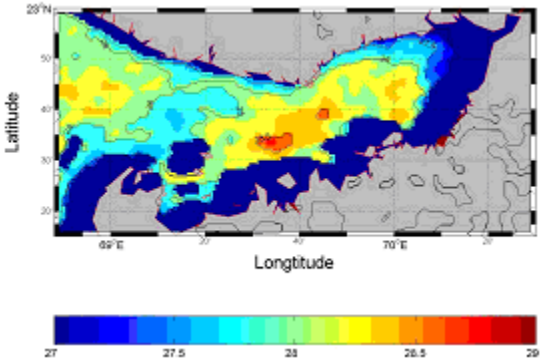

Date:07-Nov-1999 Time: 11:29 hrs

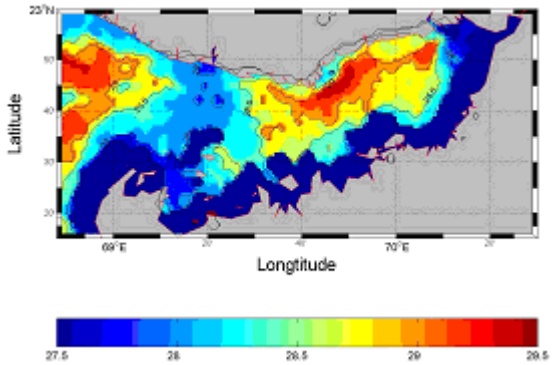

Date:11-Nov-1999 Time:10:55 hrs

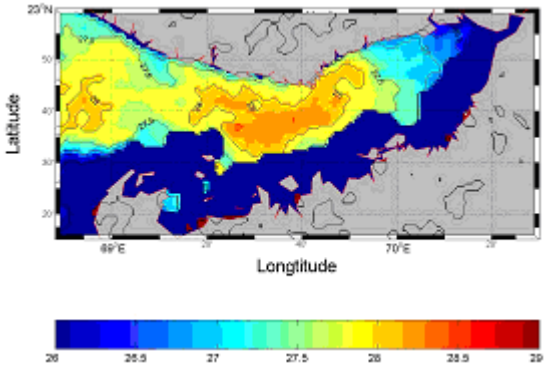

Date:19-Nov-1999 Time:11:16 hrs

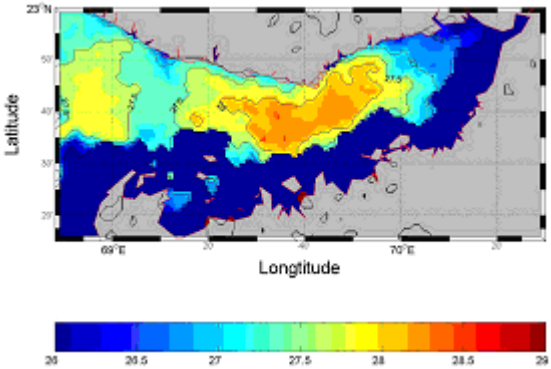

Date:20-Nov-1999 Time:11:05 hrs

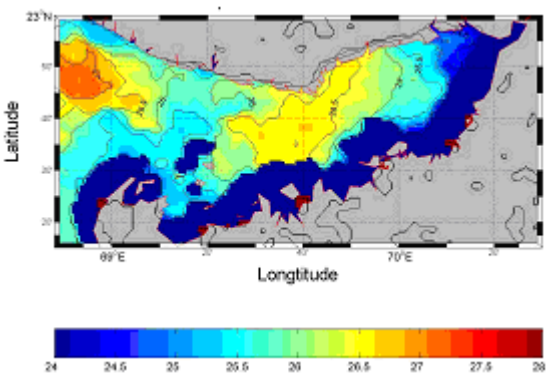

Date: 28-Nov-1999 Time:11:14 hrs

Figure. 3.9 Sea surface temperature measured by NOAA/AVHRR for 6 days of November-99

Extraction of Wind data from QuikSCAT

In this study, Wind velocity over the Gulf is retrieved from QuikSCAT satellite, which was launched in 1999 to monitor ocean wind fields globally. The scatterometer sends microwave pulses to the earth's surface and measure the backscattered power from the surface roughness. Over the ocean, the backscatter is largely due to the small centimeter waves on the surface. The idea of remote sensing of ocean surface winds was based on the belief that these surface ripples are in equilibrium with the local wind stress. The backscatter depends not only on the magnitude of the wind stress but also on the wind direction relative to the direction of the radar beam. The capability of measuring both wind speed and direction is the major uniqueness of the scatterometer. Space-based wind retrieval is largely dependent on an empirical relation between the backscatter and the equivalent neutral winds.

All wind retrieval from past and present scatterometers suffers, at various degrees, ambiguities in wind direction because of the sinusoidal relationship between the backscatter and wind direction. Measuring at the same location in different directions mitigates the problem. Wind fields from operational numerical weather forecast have usually been used as initial field for the iterative direction choosing procedures. Due to insufficient data, the relation between backscatter and wind vector under extreme conditions (high and low winds) and under heavy precipitation is less established. Strong winds and high precipitation conditions are prevalent in marine storms, but such conditions constitute only a small portion of the global wind data set.

At near-real-time, twice-daily maps of ocean surface winds over global oceans, derived from the observations by the scatterometer SeaWinds on space mission QuikSCAT, of the National Aeronautics and Space Administration (NASA) were interpolated and provided in wind grid data file (Tang and Liu,

1996) as in-situ measurements were unavailable. Figure 4.3 shows the mean wind velocity over Gulf of Kachchh from Nov.1999 to Jan. 2000. It seems that in the winter season, wind velocity over the Gulf is less than 10 m/s and wind direction are generally from North.

--- --- ---